

# Web-based Quick Estimation System of Strong Ground Motion Maps Using Engineering Geomorphologic Classification Map and Observed Seismic Records



**M. Matsuoka & N. Yamamoto**  
*Geological Survey of Japan, AIST, Japan*

## SUMMARY:

QuiQuake (**Quick** estimation system for earth**Quake** maps triggered by observation records) is a seismic event triggered quick estimation system for the generation of earthquake maps using earthquake observation records. It is a system which provides extensive and detailed strong ground motion maps such as PGA, PGV, and seismic intensity right after a seismic event in and around Japan. QuiQuake also uses the combinations of amplification capability map and observed seismic records. The amplification capability is estimated from geomorphologic conditions, based on the Japan Engineering Geomorphologic Classification Map, with spatial resolution of 7.5 arc-second and 11.25 arc-second in latitude and longitude, respectively. The automatic calculation of spatial interpolation, including consideration of the attenuation characteristic from the seismic source, is started by harvesting the seismic data recorded at strong ground motion observation stations. The strong motion maps are published online using an Open Geospatial Consortium (OGC) standard web service interface.

*Keywords: QuiQuake, Vs30, Kriging, WMS, OGC, GEO Grid*

## 1. INTRODUCTION

The GEO Grid (Global Earth Observation Grid) system (Sekiguchi et al., 2008) of the National Institute of Advanced Industrial Science and Technology, Japan (AIST) has developed a web service system for earthquake disaster response throughout Japan. The GEO Grid aims at providing integrated service using a wide array of geoscientific information such as geologic maps and other digital geographically referenced data, and assembles them into easy-to-use formats for potential stakeholders from several fields such as environmental conservation, resource exploration, hazard evaluation, and risk management. To provide these services, AIST set up web-based systems using Grid and Web service technologies in accordance with international standards. In order to take effective countermeasures against seismic disasters and implement business continuity plans (BCPs) for municipalities and private companies, the quick estimation of strong ground motions is very essential at the early stages of disaster response activities (e.g. Yamazaki et al., 1998; Ariki et al., 2004). QuiQuake (**Quick** estimation system for earth**Quake** maps triggered by observation records) is a seismic event triggered quick estimation system for the generation of earthquake maps using earthquake observation records. It is one of the geological hazard related applications on GEO Grid and the first system which estimates and illustrates the extensive and detailed ground motion maps such as peak ground acceleration (PGA), peak ground velocity (PGV), and JMA (Japan Meteorological Agency)-scale instrumental seismic intensity ( $I_{JMA}$ ), right after an earthquake occurs. In this system, an amplification capability of ground motion and Vs30 average shear-wave velocity map, which is estimated from a 250-m grid cell map of the Japan Engineering Geomorphologic Classification Map (JEGM) (Wakamatsu and Matsuoka, 2011), are also used for the spatial interpolation calculation to generate strong motion maps. The interpolation also takes into account the characteristics of soil conditions. The strong ground motion maps are automatically calculated and published through an Open Geospatial Consortium (OGC) standard web service interface, right after the seismic observation data are released by the National Research Institute for Earth Science and Disaster Prevention (NIED). In this paper, we present the outline of QuiQuake, the data and

algorithms used to generate strong ground motion maps.

## 2. OUTLINE OF QUIQUAKE AND CALCULATION PROCEDURE

Data flow and spatial interpolation procedure are shown in Fig. 1. The QuiQuake generates two kinds of strong ground motion maps with 250-m spatial resolution. The first one is QuakeMap which is calculated using the published seismic observation records at the portal site of the NIED. The second map is the QuickMap which is an output of quick estimation system. It is calculated using the near real-time information of strong ground motion parameters delivered by NIED right after an earthquake. Both maps are generated and published automatically using parallel computing techniques implemented by AIST's GEO Grid computer clusters.

The first phase of the generation of the ground motion maps is the processing of the near real-time observation data from K-NET (Kyoshin network). The ground motion parameters at the recording stations were assigned to the amplification capabilities estimated from the average shear-wave velocity of the ground in the upper 30 m ( $V_{s30}$ ). The data are then converted to a base-rock level ( $V_{s30} = 600$  m/s) by using amplification factors. Since the earthquake motion on the ground surface is affected by the amplification characteristics of surface layers, the spatial interpolation by IDW (Inverse Distance Weighted) is carried out at the base-rock (outcrop) level. Finally, the spatial distributions of the ground motion parameters such as PGA, PGV, and  $I_{JMA}$  on the ground surface are obtained by multiplying the corresponding amplification factor for each grid cell. Following the aforementioned procedure, QuickMap could be generated.

When seismic waveform records at seismic stations from the K-NET and KiK-net (Kiban Kyoshin network) are published at the portal site, QuakeMap generation starts. The data are downloaded automatically and ground motion parameters, PGA, PGV, and  $I_{JMA}$  at the stations are calculated. Using the application factor, the parameters recorded on the surface are converted to values at the base rock level. For QuakeMap, one of the stochastic interpolation methods, called "Simple Kriging" with a prior trend component, is used to estimate the spatial distributions of ground motion parameters at the base rock level. The trend component is assigned for the attenuation relation obtained at the ground base level for each seismic event based on the location of the epicentre. PGA, PGV, and  $I_{JMA}$  maps on the ground surface are finally calculated by multiplying the amplification factors.

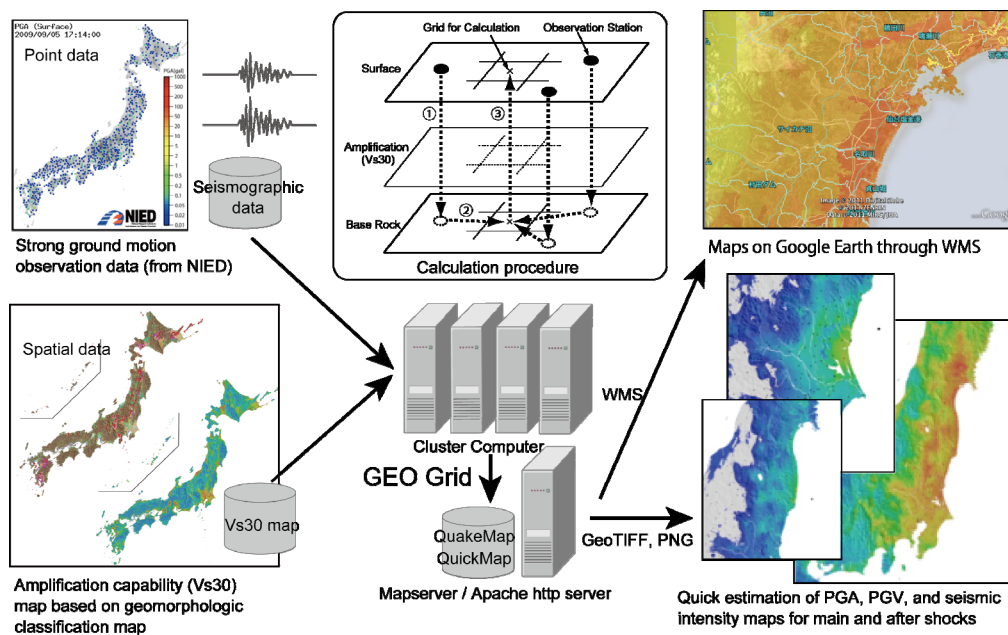


Figure 1. System overview and calculation procedure

### 3. GROUND CONDITION AND AMPLIFICATION CAPABILITY MAPS

Local geologic and ground conditions play important roles in characterizing and estimating the site amplification capability of strong ground motion and geotechnical hazards. Accurate evaluation of site amplification characteristics requires detailed soil profile information such as the data on shear-wave velocity structures. However, high-density boring or PS-logging data throughout Japan are not available. It has been determined that approximate estimation of site amplification is possible using the average shear-wave velocity of ground in the upper 30 meters, also known as Vs30 (Borcherdt and Gibss, 1976; Joyner and Fumal, 1984; Midorikawa et al., 1994). Estimating Vs30s covering wider area could be done using surface geology and/or geomorphologic conditions, and digital elevation model. A product of Earthquake Hazard Program, ShakeMap, developed by the U.S. Geological Survey (USGS) uses Vs30 map for the key parameter to estimate site amplification characteristics (Wald et al., 2005). The QuiQuake also uses Vs30 as an amplification parameter and Japan Engineering Geomorphologic Classification Map (JEGM) for the source of ground condition data.

#### 3.1. 7.5-arc-second JEGM

The map contains an attribute of geomorphologic land classification in grid cells that are 7.5 arc-seconds latitude  $\times$  11.25 arc-seconds longitude in size (approximately 250  $\times$  250 m<sup>2</sup>). A description of geomorphologic map units is presented in Table 1, together with the corresponding general ground conditions and general depth of groundwater. These criteria were based on the purpose of the mapping project, the identification and classification of subsurface ground conditions using standard geomorphologic classification. The geomorphologic factors presented in Table 1 are known to be correlated with subsurface ground and hydrologic conditions (e.g. Zuidam, 1986). Figure 2(a) shows a sample image of the 7.5-arc-second JEGM overlaid on the shade map created from the digital elevation model covering the entire country of Japan. The total number of cells of the map is approximately 6 million.

**Table 1.** Description of geomorphologic map units in the 7.5-arc-second JEGM

Geomorphologic map unit	Definition and general characteristics	Subsurface soil condition	General depth of groundwater*
Mountain	Steeply to very steeply sloping topography with highest elevation and relative relief within a grid cell of more than approximately 200 m. Moderately to severely dissected.	Pre-Quaternary hard to soft rock.	Deep
Mountain footslope	Gently sloping topography adjoining mountains and composed of material sourced from the mountains such as colluvium, talus, landslide, and debris flow deposits.	Loose debris and soils consisting of colluvium, talus, landslide, and debris flow deposits.	Deep
Hill	Steeply to moderately sloping topography with higher elevation and relative relief within a grid cell of approximately 200 m or less. Moderately dissected.	Pre- Quaternary and Quaternary hard to soft rock.	Deep
Volcano	Steeply to moderately sloping topography with higher elevation and larger relative relief, composed of Quaternary volcanic rocks and deposits.	Quaternary hard to soft volcanic rock and/or deposits.	Deep
Volcanic footslope	Gently sloping topography located around skirt of volcano including pyroclastic-, mud- and lava-flow fields, and volcanic fan produced by	Quaternary loose to dense volcanic deposits consisting of ash, scoria, pumice, pyroclastic flow, lava, debris	Deep

	dissection of volcanic body. Slightly dissected.	avalanche, etc.	
Volcanic hill	Moderately sloping topography composed of pyroclastic flow deposits. Moderately to severely dissected.	Loose to moderately loose pyroclastic flow deposits such as ash, scoria, and pumice.	Deep
Rocky strath terrace	Fluvial or marine terrace with flat surface and step-like form, including limestone terrace of emerged coral reef. Thickness of subsurface soil deposits is less than 5 m.	Hard to soft rock.	Deep
Gravelly terrace	Fluvial or marine terrace with flat surface and step-like form. Covered with subsurface deposits (gravel or sandy soils) more than 5 m thick.	Dense gravelly soil.	Deep
Terrace covered with volcanic ash soil	Fluvial or marine terrace with flat surface and step-like form. Covered with cohesive volcanic ash soil to more than 5 m thick.	Stiff volcanic ash (cohesive soil).	Deep
Valley bottom lowland	Long and narrow lowland formed by river or stream between steep to extremely steep slopes of mountain, hill, volcano, and terrace.	Moderately dense to dense gravel or boulders in mountain, but loose sandy soil to very soft cohesive soil in plain.	Shallow
Alluvial fan	Semi-cone-like form composed of coarse materials, which is formed at the boundary between mountains and lowland. Slope gradient is more than 1/1000.	Dense gravel with boulders to moderately dense sandy gravel.	Deep in the central part of fan but shallow in the distal part of fan
Natural levee	Slightly elevated area formed along the riverbank caused by fluvial deposition during floods.	Loose sandy soil.	Shallow
Back marsh	Swampy lowland formed behind natural levees and lowlands surrounded by mountains, hills, and terraces.	Very soft cohesive soil containing peat or humus.	Very shallow
Abandoned river channels	Swampy shallow depression along former river course with elongated shape.	Very loose sandy soil occasionally covered with soft cohesive soil.	Very shallow
Delta and coastal lowland	Delta: flat lowland formed at the river mouth by fluvial accumulation. Coastal lowland: flat lowland formed along shoreline by emergence of shallow submarine deposits, including discontinuous lowlands along sea- or lake- shore.	Loose fluvial sandy soil over-lying very soft cohesive soil.	Shallow
Marine sand and gravel bars	Slightly elevated topography formed along shoreline, composed of sand and gravel, which was washed ashore by ocean wave and/or current action.	Moderately dense to dense marine sand or gravel occasionally with boulder.	Shallow
Sand dune	Wavy topography usually formed along shoreline or river, comprised of fine to moderately aeolian sand; generally	Very loose to loose fine to medium sand.	Deep at crest of dune but shallow

	overlies sandy lowland.		near base of dune
Lowland between coastal dunes and/or bars	Swampy lowland formed behind dunes or bars	Very soft cohesive soil containing peat or humus.	Very shallow
Reclaimed land	Former bottom flat of sea, lake, lagoon, or river that has been reclaimed as land by drainage.	Loose sand overlying very soft cohesive soil, sometimes covered with loose sandy fill.	Very shallow
Filled land	Former water body such as sea, lake, lagoon, or river reclaimed as land by filling.	Very loose to loose sandy fill, overlying very soft cohesive soil or loose sandy soils.	Very shallow to shallow
Rock shore, Rock reef	Irregular topography of rock or coral around beach zone.	Pre- Quaternary and Quaternary hard to soft rock	Near sea level
Dry riverbed	Nearly flat, irregular topography without water in normal time.	Loose sandy to gravelly alluvial soil, occasionally with boulders.	Very shallow
River bed	Nearly flat, irregular topography with varying water cover and having erosion and accumulation parts.	Loose sandy to gravelly alluvial soil, occasionally with boulders	
Lake	Inland water body.		
Nearshore waters	Nearshore water body.		

\* Deep: deeper than 3 m below the ground surface, Shallow: within 3 m of the ground surface, Very shallow: within 1 m of the ground surface

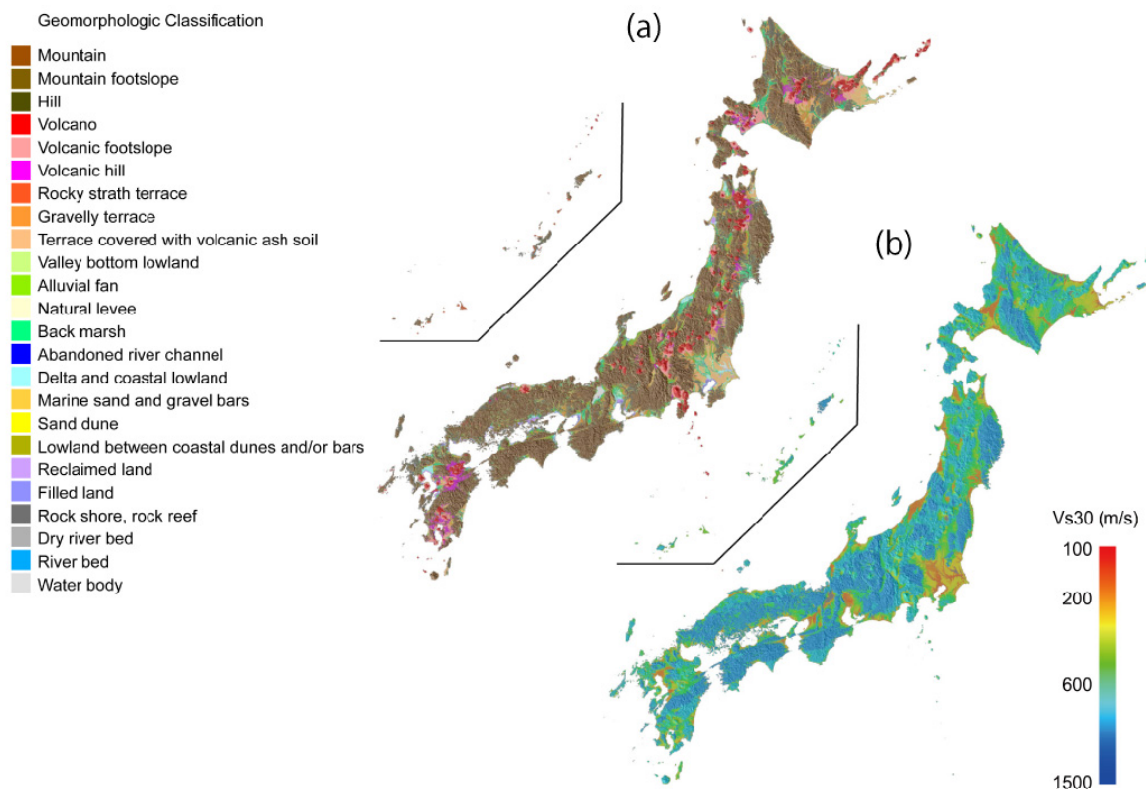


Figure 2. (a) 7.5-arc-second JEGM and (b) Vs30 map

### 3.2. Average Shear-wave Velocity ( $V_{s30}$ ) and Amplification Capabilities

The  $V_{s30}$  values covering approximately 2,000 sites all over Japan were calculated from a previous study (Matsuoka et al., 2006). Geomorphologic units for all PS-logging data sites were interpreted. Then the correlation between geomorphologic units and geographical information derived from the JEGM and the  $V_{s30}$  values were examined. It was found that the  $V_{s30}$ s showed some dependency on altitudes, slopes, and distances from mountains or hills formed during older periods (Pre-Tertiary or Tertiary). Based from this observation, a multiple linear regression formula for each geomorphologic unit was developed to estimate the  $V_{s30}$  using elevation ( $Ev$ ), slope ( $Sp$ ), and distance ( $Dm$ ) from a mountain or a hill as explanatory variables. The basic regression formula is

$$\log V_{s30} = a + b \log Ev + c \log Sp + d \log Dm \pm \sigma \quad (1)$$

where  $a$ ,  $b$ ,  $c$ , and  $d$  are regression coefficients, and  $\sigma$  as the standard deviation. The units of  $Ev$ ,  $Sp$ , and  $Dm$  are meters, 1000 times tangent values, and kilometers, respectively. When the value of the explanatory variable is less than 1, we fixed the value as 1. Table 2 shows the regression coefficients and standard deviation of each geomorphologic unit obtained by regression analysis. The regression coefficients show that the higher is the elevation, the steeper is the slope. On the other hand, the shorter the distance from the mountain or hill the higher is the  $V_{s30}$ .

**Table 2.** Regression coefficient of Eqn. 1 (Matsuoka et al., 2006)

Geomorphologic map unit	$a$	$b$	$c$	$d$	s.d.
Mountain (Pre-Tertiary)	2.900	0	0	0	0.139
Mountain (Tertiary)	2.807	0	0	0	0.117
Mountain footslope	2.602	0	0	0	0.092
Hill	2.349	0	0.152	0	0.175
Volcano	2.708	0	0	0	0.162
Volcanic footslope	2.315	0	0.094	0	0.100
Volcanic hill	2.608	0	0	0	0.059
Rocky strath terrace	2.546	0	0	0	0.094
Gravelly terrace	2.493	0.072	0.027	-0.164	0.122
Terrace covered with volcanic ash soil	2.206	0.093	0.065	0	0.115
Valley bottom lowland	2.266	0.144	0.016	-0.113	0.158
Alluvial fan	2.350	0.085	0.015	0	0.116
Natural levee	2.204	0.100	0	0	0.124
Back marsh	2.190	0.038	0	-0.041	0.116
Abandoned river channel	2.264	0	0	0	0.091
Delta and coastal lowland	2.317	0	0	-0.103	0.107
Marine sand and gravel bars	2.415	0	0	0	0.114
Sand dune	2.289	0	0	0	0.123
Reclaimed land	2.373	0	0	-0.124	0.123
Filled land	2.404	0	0	-0.139	0.120

The  $V_{s30}$  distribution with 250 m spatial resolution was computed using Eqn. 1 and the attributes of the geomorphologic classification in the 7.5-arc-second JEGM, together with the geologic age, elevation, and slope values. Figure 2(b) shows the  $V_{s30}$  map covering Japan. The  $V_{s30}$  values are approximately 150 m/s on delta and coastal lowland, reclaimed land and back marsh. The areas covering valley bottom lowland also show a rather small  $V_{s30}$  ranging from 180 to 200 m/s. To draw amplification capability maps,  $V_{s30}$  was converted into the amplification factors for PGA, PGV, and  $I_{JMA}$  with respect to stiff soil, which corresponds to grounds with  $V_{s30}$  of 600 m/s, using the empirical relationships (Fujimoto and Midorikawa 2006; Midorikawa et al., 2008).

## 4. PUBLICATIONS AND VERIFICATION

### 4.1. Portal Site and OGC Standards Publishing

The QuickMap results are generally available within 5 minutes after the occurrence of a 7.0 magnitude earthquake on QuiQuake homepage (<http://qq.ghz.geogrid.org/QuickMap/index.en.html>). Figure 3 shows the QuickMap portal site. The 8-bit unsigned integer GeoTiff file, which can be converted to the physical value of ground motion parameters, is downloadable from the site. Since calculation area is automatically determined to include the observation points where shaking occurred, the computation time is dependent on the magnitude of an earthquake. The automatic delivery of a message on Twitter (@QuiQuake) by “BOT” notifies that QuickMap is already available (see in Fig. 4). The QuakeMap, which take longer computation time than QuickMap, are also released on the homepage (<http://qq.ghz.geogrid.org/QuakeMap/index.en.html>). Furthermore, QuakeMap results for more than 7,500 major earthquakes after June 1996 have been computed and archived such that they chronologically represent the seismic motions over the last 15 years.

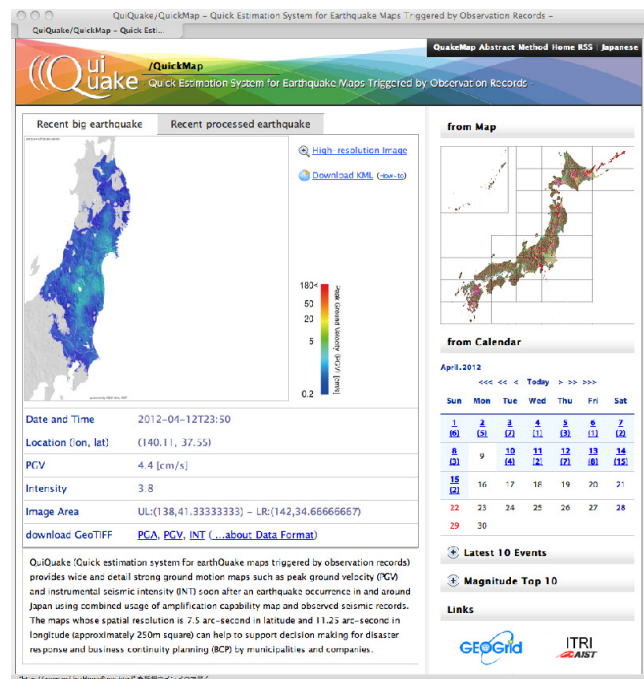


Figure 3. QuickMap portal site (<http://qq.ghz.geogrid.org/QuickMap/index.en.html>)

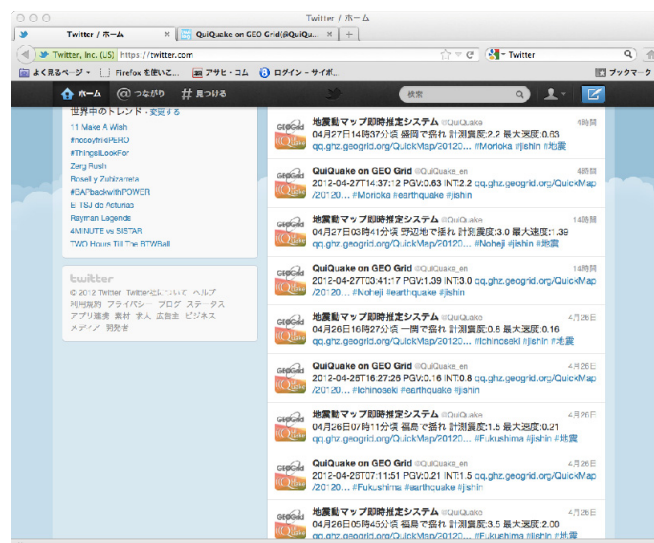
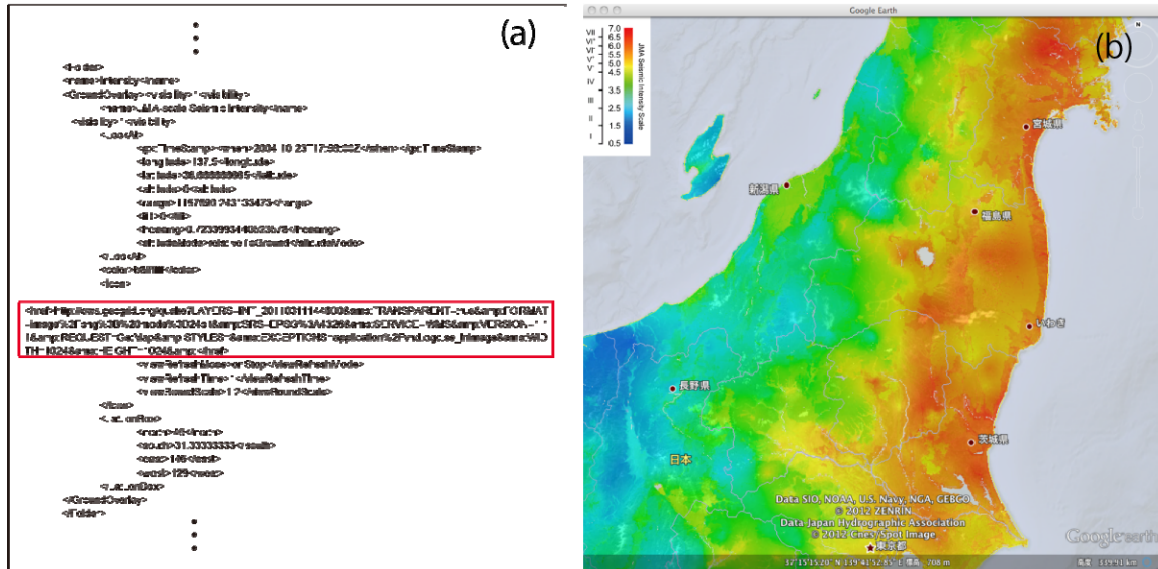


Figure 4. QuickMap twitter log (@QuiQuake)

Earth observation data, such as strong motion observation records, shake maps, geological conditions, and remote sensing imagery are GIS based data that can be fully utilized through synergy with other GIS data available on the Internet. The most widely accepted standards are OGC (Open Geospatial Consortium) specifications such as the Web Map Service (WMS), tWeb Feature Service (WFS), and the Web Coverage Service (WCS). Since the QuickMap and QuakeMap contain information on each location-based grid-cell, it was decided to disseminate the maps using WMS/WCS. The example of KML document with WMS URI of QuakeMap imagery of the  $I_{JMA}$  distribution covering the 2011 Tohoku, Japan earthquake affected area is displayed on Google Earth as shown in Fig. 5.



**Figure 5.** (a) Example of KML document containing the WMS URI of QuakeMap imagery. Red rectangle highlights the inserted WMS URI. (b) Spatial distribution of  $I_{JMA}$  of the 2011 Tohoku earthquake overlaid on Google Earth platform.

#### 4.2. Verification of QuakeMap Results

The accuracies of the estimated  $I_{JMA}$  in QuakeMap using strong motion observation records from other organizations' networks during the recent nine earthquakes; the 2000 Tottori-ken-seibu, the 2003 Miyagi-ken-oki, the 2003 Miyagi-ken-hokubu, the 2003 Tokachi-oki, the 2004 Niigata-ken Chuetsu, the 2005 Fukuoka-ken-seiho, the 2007 Noto-hanto-oki, the 2007 Niigata-ken Chuetsu-oki, and the 2008 Iwate-Miyagi-nairiku earthquakes were determined (Matsuoka et al., 2011). As in described in Section 2, ground motion values were estimated based on Simple Kriging of the K-NET and KiK-net data and the amplification capability estimated from the Vs30. The estimated  $I_{JMA}$  values were compared with observed  $I_{JMA}$  values recorded at seismic stations owned by other organizations, such as the JMA, the Port and Airport Research Institute, the Central Research Institute of Electric Power Industry, the East Japan Railway Company, the NEXCO East, and the Committee of Earthquake Observation and Research in the Kansai Area. The standard deviation of estimation error (residual of the estimated and actual values) from the nine earthquakes is approximately 0.5 in  $I_{JMA}$ . Figure 6 shows the comparison for the 2004 Niigata-ken Chuetsu earthquakes. A relatively good agreement between the observed values and the estimated ones in QuakeMap is observed.

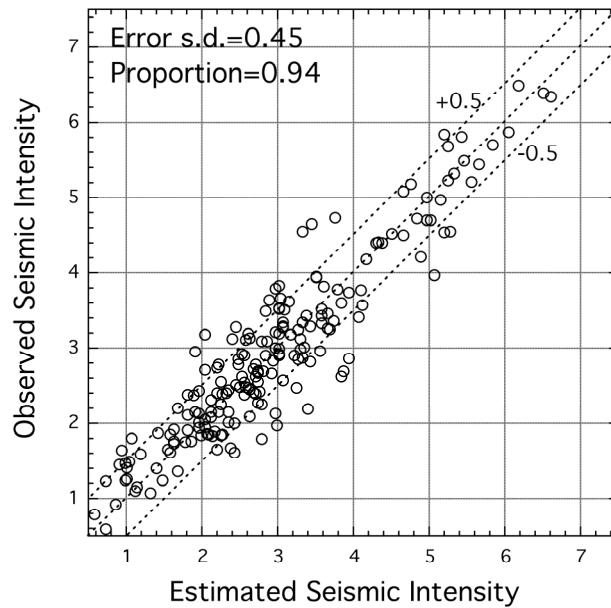


**Figure 6.** Comparison of the observed ground motion recorded by other organizations' seismic network stations and the estimated values at the stations estimated by Kriging using K-NET and KiK-net sites, and the amplification capability from Vs30 map for the 2004 Niigata-ken Chuetsu earthquake (Matsuoka et al., 2011)

## 5. CONCLUSIONS

This paper outlines the components of the QuiQuake, which provides a 250-m resolution strong ground motion maps covering wide area, for quick disaster response right after an earthquake occurrence throughout Japan, is presented. In this system, an amplification capability map of ground motion (Vs30 map) based on Japan Engineering Geomorphologic Classification Map (JEGM) and seismic observation records from K-NET and KiK-net released by the National Research Institute for Earth Science and Disaster Prevention (NIED) are processed on a GEO Grid cluster computer of AIST. The use of the GEO Grid system in producing strong ground motion maps offers the following advantages: a) fully automatic, quick, and multi-task computing for mainshock and continued aftershocks, b) publication of the maps through Open Geospatial Consortium (OGC) compliant Web GIS server, and c) possibility to expand more stabilized and redundant operations by Virtual Machine in external servers and Cloud system.

## ACKNOWLEDGEMENT

The QuiQuake system is supported by the National Research Institute for Earth Science and Disaster Prevention (NIED), the Japan Nuclear Energy Safety Organization (JNES), and ITOCHU Techno-Solutions Corporation (CTC). The system uses the data records of strong motion network (K-NET and KiK-net) administrated by NIED and the published program of Prof. Y. Hisada, Kogakuin University, to calculate instrumental seismic intensity. Prof. K. Wakamatsu of Kanto Gakuin University cooperated the Vs30 map creation. "RAPID Shake Map simulator with Observed records (RASMO)" which was developed by Dr. I. Suetomi, Eight-Japan Engineering Consultants Inc. and Mr. M. Hashimoto, Kozo Keikaku Engineering Inc. and published by Kawasaki Laboratory, NIED is used for interpolation calculation. We optimized the software for fast calculation in the GEO Grid system. For validation of the system, we used the data from the JMA, the Port and Airport Research Institute, the Central Research Institute of Electric Power Industry, the East Japan Railway Company, the NEXCO East, and the Committee of Earthquake Observation and Research in the Kansai Area. To all of the aforementioned scientists and organizations, we would like to express our gratitude.

## REFERENCES

Ariki, F., Shima, S. and Midorikawa, S. (2004). Earthquake disaster prevention of Yokohama City. *Journal of*

- Japan Association for Earthquake Engineering* **4:3**, 148-153.
- Borcherdt, R.D. and Gibbs, J.F. (1976). Effects of local geological conditions in the San Francisco bay region on ground motions and the intensities of the 1906 earthquake. *Bulletin of Seismological Society of America* **66:2**, 467-500.
- Fujimoto, K. and Midorikawa, S. (2006). Relationship between average shear-wave velocity and site amplification inferred from strong motion records at nearby station pairs. *Journal of Japan Association for Earthquake Engineering*. **6:1**, 11-22 (in Japanese with English abstract).
- Joyner, W.B. and Fumal, T.E. (1984). Use of measured shear-wave velocity for predicting geologic and site effects on strong ground motion. *8th World Conference on Earthquake Engineering*. **Vol.2:** 777-783.
- Matsuoka, M., Wakamatsu, K., Fujimoto K. and Midorikawa, S. (2006). Average shear-wave velocity mapping using Japan Engineering Geomorphologic Classification Map. *Journal of Structural Engineering and Earthquake Engineering*. **23:1**, 57s-68s.
- Matsuoka, M., Wakamatsu, K. and Hashimoto, M. (2011). Liquefaction potential estimation Based on the 7.5-arc-second Japan Engineering Geomorphologic Classification Map, *Journal of Japan Association for Earthquake Engineering*. **11:2**, 20-39 (in Japanese with English abstract).
- Midorikawa, S., Matsuoka, M. and Sakugawa, K. (1994). Site effects on strong-motion records observed during the 1987 Chiba-ken-toho-oki, Japan earthquake. *9th Japan Earthquake Engineering Symposium*. **Vol.3:** 85-90.
- Midorikawa, S., Komazawa, M. and Miura, H. (2008). Relationships between average shear-wave velocity and site amplification factors obtained by records from Yokohama dense strong-motion network. *Journal of Japan Association for Earthquake Engineering*. **8:3**, 19-30 (in Japanese with English abstract).
- Open Geospatial Consortium (OGC). Available: <http://www.opengeospatial.org/> (Access on 1 April, 2012)
- Sekiguchi, S., Tanaka, Y., Kojima, I., Yamamoto, N., Yokoyama, S., Tanimura, Y., Nakamura, R., Iwao, K. and Tsuchida, S. (2008). Design principles and IT overviews of the GEO Grid. *IEEE Systems Journal* **2:3**, 374-389.
- Wakamatsu, K. and Matsuoka, M. (2011). Developing a 7.5-sec site-condition map for Japan based on geomorphologic classification. *Earthquake Resistant Engineering Structures VIII, WIT Press*: 101-112.
- Wald, D.J., Worden, B.C., Quitoriano, V., and Pankow, K.L. (2005). ShakeMap Manual: Technical Manual, User's Guide, and Software Guide, U.S. Geological Survey, USA.
- Yamazaki, F., Noda, S. and Meguro, K. (1998). Developments of early earthquake damage assessment systems in Japan. *Structural Safety and Reliability, ICOSSAR '97*: 1573-1580.
- Zuidam, R.A.van (1986). Aerial Photo-Interpretation in Terrain Analysis and Geomorphologic Mapping, Smits Publishers, Hague.